RESEARCH ARTICLE OPEN ACCESS

Study on hardening mechanisms in aluminium alloys

P. K. Mandal
Department of Metallurgical and Materials Engineering, Indian Institute of Technology Roorkee (IITR),Roorkee, UK-247667, INDIA

Abstract
The Al-Zn-Mg alloys are most commonly used age-hardenable aluminium alloys. The hardening mechanism is further enhanced in addition of Sc. Sc additions to aluminium alloys are more promising. Due to the heterogeneous distribution of nano-sized Al_3Sc precipitates hardening effect can be accelerated. Mainly, highlight on hardening mechanism in Al-Zn-Mg alloys with Sc effect is to study. In addition, several characterisations have been done to age-hardening measurements at elevated temperatures from 120^{o}C to 180 ^{o}C. The ageing kinetics has also been calculated from Arrhenius equation. Furthermore, friction stir processing (FSP) can be introduced to surface modification process and hardened the cast aluminium alloys. In this study, hardening mechanism can be evaluated by Vicker's hardness measurement and mechanical testing is present task.

Key words: hardening mechanism, Al_3Sc precipitates, ageing kinetics, Arrhenius equation, FSP, mechanical testing.

I. Introduction

Aluminium alloys are more promised light weight for the application to automobiles, air crafts and various machine components. Their mechanical property has been improved by the strong age-hardening their heat treatment. The precipitation process in Al-base alloys indicates a several transformation sequences during ageing. Heat treatment relies on the fine precipitation from the supersaturated solid solution (SSS), and precipitation is associated with nucleation and growth process. Since, aluminium alloys are age hardening phase as taken account through the activation energy for ή nucleation and its precursors [1]. It is also taken account through transition element, Sc addition and its effect during ageing kinetics in these alloys.Therefore, it becomes essential to control nanoscale precipitates in aluminium alloys. The nano-clusters are expected to act as effective heterogeneous nucleation sites for the subsequent precipitates and affect microstructures and resultant alloy properties.In case of Sc added alloys, mechanism of increasing strengthening effect has been considered as additional hardening by precipitated Al_3Sc, restraint of recrystallization, promotion of nucleation of ή particle and restraint of η coarsening.Dritz and co-workers investigated the connection between precipitates and mechanical properties in Al-Sc alloys with 0.1 to 0.8 wt% Sc concentrations. They found that the maximum value of the yield stress increased monotonically with the increasing Sc content [2, 3]. The work-hardening process has been studied in 7XXX series of aluminium alloys and described by Holloman equation, $\sigma = K\varepsilon^n$ ……(1)Where σ and ε are the true stress and true strain, respectively. The constants K and n are assumed to be independent of strain [4, 5].It is also pointed out in literature, that the considerable improvement in strength of aluminium alloys can be achieved by precipitation hardening, as several demonstrations Osamura et al, Kovacs et al and poole et al have shown. They investigated the relationship between the duration of the ageing treatment and mechanical properties of polycrystalline 7000-type aluminium alloys [6].Recently, FSP has been shown to be a feasible technique to produce large-area thin plate of ultrafine grained 7XXX series of aluminium alloys. Due to the severe deformation and short time at elevated temperature in FSP as well as the presence of a considerable amount of second phase, grain growth could be limited effectively in the dispersoids studied here. Therefore, it is possible to further refine and homogenize the structure and to produce large volume of materials by applying double passes of FSP [6,7].Hence, the objective of this work which is to study the response of the alloy system to age hardening heat treatment in terms of mechanical properties.

II. Experimental procedure

The four types of alloys were produced through cast metallurgy. The melting was done using a muffle resistance furnace at fixed temperature, 780 ^{o}C. During melting as following steps was followed- at Step-1, pure Al heated up at above temperature for two hours in graphite crucible (capacity 2.5 kgs.), then Al-2%Scmaster alloy added and kept for half an hour. At Step-2, hot crucible brought out side from the furnace and plungedpure Mg, pure Zn in liquid metal gradually,cautiously. At Step-3, slag removed

from top of the melt and poured into metallic mouldquickly. The following cast samples was kept in room temperature for seven days then preferred for solution treatment at 465 ^{o}C for one hour and water quenched immediately. The following solution treated samples was kept for three days in room temperature then preferred for artificial ageing treatment at 120^{o}C, 140^{o}C, and 180 ^{o}C, respectively. During, each ageing treatment was tabulated Vicker's hardness (FIE-VM50 PC) data using 10 kgf and 15 seconds dwell time at different time interval up to twenty hours.The each experimental hardness was shorted out at average five indentations. The cast alloys was selected for optical microscopy and TEM (transmission electron microscopy) slice with 3 mm diameter were cut as from the as-cast 10×10 mm^2 discs and thickness reduced to 0.1 mm by disc polisher. Then, the TEM samples were prepared using twin-jet electro-polishing (solution was 75% CH_3OH and 25% HNO_3) at 12 V and -35 ^{o}C. All the imaging was carried out using at Techai G^2 20 S-TWIN at 200 kV. The solution treated samples were selected for FSP (friction stir processing) by double passesand all parameters were tabulated (in Table-4) during metal processing.In Fig.-1, the FSP set-up is shown and plate dimension 150× 90×6 mm^3 with tool rotation speed 1000 rpm with clockwise direction maintain. The tensile tests were carried out by using an Instron testing machine at a cross head speed of 1 mm/min. The tensile specimen having dimensions 26 mm gauge length, 4 mm width, 2.5 mm thickness and 58 mm full length. The tensile test samples were collected from stir zone and machined as per following standard dimensions (in Fig.-1).

Table-1: Chemical composition analyzed by ICP-AES and AAS methods of studied alloys (wt.%).

Alloy no.	Zn	Mg	Sc	Si	Fe	Al	Zn+Mg	Zn/Mg
Alloy-1	6.5	2.9	-	0.01	0.05	Bal.	9.4	2.2
Alloy-2	8.3	3.3	-	0.02	0.04	Bal.	11.6	2.5
Alloy-3	5.3	3.0	0.25	0.11	0.10	Bal.	8.3	1.8
Alloy-4	7.1	3.2	0.83	0.01	0.03	Bal.	10.3	2.2

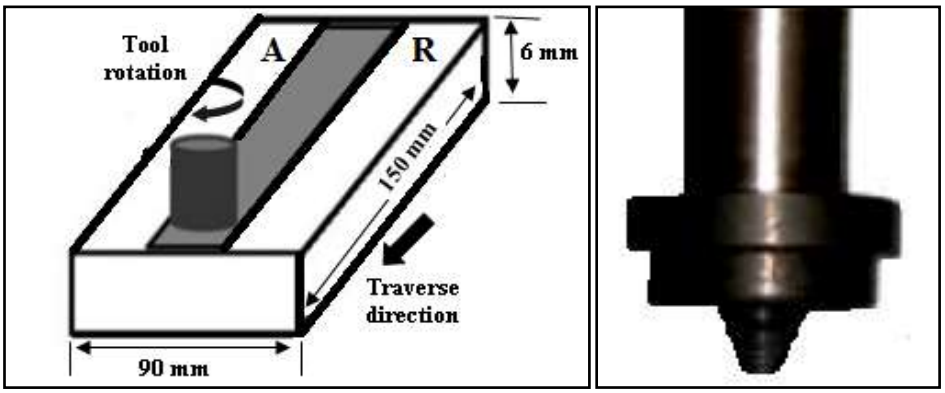

Fig.-1: Schematic illustration of the friction stir processing (FSP) and tool pin.

Table-2: FSP tool characteristics and process parameters.

Shoulder diameter (mm)	25
Pin diameter (mm)	5
Pin height (mm)	3.5
Clockwise, tool rotation speed (rpm)	1000
Plate travel speed (mm/min)	75
Friction pressure, (up-setting force, KN)	15
Pin angle (^{o})	2.5
Number of passes	two
Plate dimension	150× 90×6 mm^3

III. Results and discussion

In study alloys, Al-Zn-Mg is display a very good age hardening. The precipitation hardening sequence of this system can be condensed in the following formulas: SSSS → GP(GP-I and GP-II) + VRC → ή → η …….(2); where the supersaturated solid solution (SSSS) is obtained after solution treatment and quenching. Depending on the composition and the dimension of the solute atoms different kinds of coherent Guinier-Preston zones (GP) could be formed. VRC are vacancy rich clusters of Zn[9]. The intermediate precipitates are the semicoherent phase ή and η($MgZn_2$) is the stable phase of each alloy. The transformation from ή to η takes place gradually in

water quenched alloys. After quenching, a typical aluminium alloy has a vacancy supersaturation of the order of 10^{10} per cm^2, i.e., much greater than the solute super- saturation. The excess vacancies tend to precipitate as loops, helices and possibly small clusters.It is characterized by the change in particle morphology from plates to laths. The mechanism of nucleation of precipitates from supersaturated solid solutions is of considerable importance since it determines the scale of the precipitates dispersion which is the most factors in determining the properties of the heat treated alloy [10].Moreover, Mg is a very useful addition to Al-Zn-Mg alloy in that it reduces their density while at the same time increasing strength and corrosion resistance. For Zn is an important element in the high strength of this alloy. The hardenability of these alloys is a result of the precipitation of an intermediate semicoherent phase based on ή($MgZn_2$), which is does not produce internal coherency strains. The hardening mechanism is in simply dispersion hardening. During ageing Al-Zn-Mg alloys, the segregated elements form $MgZn_2$ and a consequence, there exists a precipitation free zone (PFZ) at both side of the grain boundary. In additions of Sc in aluminum cause a very strong hardening effect and formed Al_3Sc, intermetallic in the Al-Sc phase diagram, this intermetallic having the same FCC crystalline lattice as Al, and parameters of their lattices differ only by 1.3%. The solubility of Sc in Al at the melting point of Al is approximately 0.3 at.% and sharply decreases while cooling. It conditions the possibility for the creation of a supersaturated solid solution by quenching and the precipitation of very disperse particles of Al_3Sc type, which are coherently bound to matrix, during ageing. The size of disperse Al_3Sc particles after ageing at the temperature close to 300 ^oC is usually about several nanometers (3 to 0.5), which just causes a very strong hardening. Also, Sc has several the beneficial effects to precipitated Al_3Sc forms smaller crystals and the volume of precipitation free zones are reduced [11]. The precipitation hardening or age hardening is a thermal treatment, which consists of a solution treatment, quenching and artificial ageing processes. For ageing processes, the specimens were aged by artificial ageingtemperatures, 120to 180 ^oC

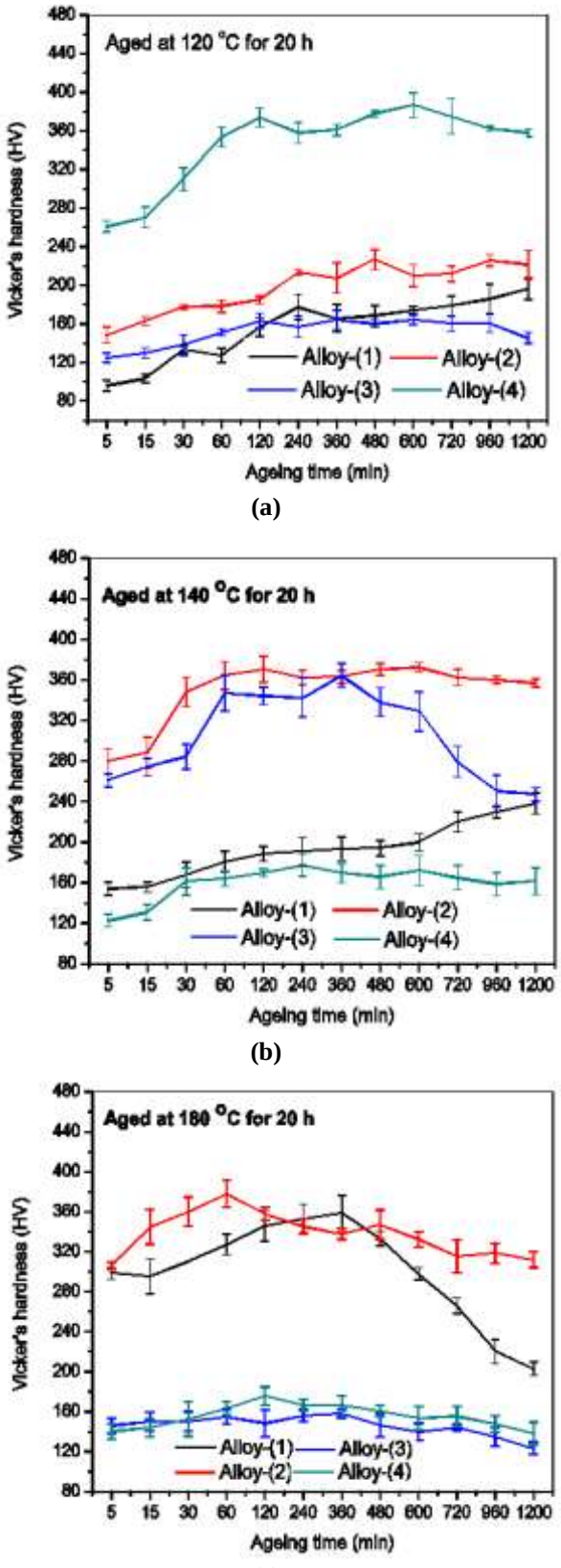

Fig.-2: Variation in the Vicker's hardness with artificial ageing time (min) for the studiesAlloys: (a) 120 ^oC, (b) 140 ^oC, and (c) 180 ^oC.

betweena few minutes to few hours. Time and temperature were two variables during hardness study. A total of five readings were taken for every ageing time at the respective temperatures and average value was tabulated.In addition, the Vicker's hardness test is to evaluate the hardness of aluminium alloys during ageing processes. In Fig.-2(a) shows at 120 ^{o}C ageing phenomena, that the hardness of the alloys increased gradually from under aged region to peak aged region. However, it decreased over aged region. For alloy alloy-2 and alloy-4, rapid hardening occurred in 2 h ageing time, because in alloy-2 high solute content (Zn+Mg = 11.6) and in alloy-4 high Sc content 0.83%. This temperature range usually called GP zones formation region that can be accelerated with high solute content and high Sc content, respectively.Rest of the two alloys (alloy-1 and alloy-3) showed normal age hardening effect.In Fig.-2(b) shows at 140 ^{o}C ageing phenomena, that the hardness of alloys (Alloy-2& Alloy-3) peak hardening reached in 1 h ageing time,because in alloy-2 solute content high and in alloy-3 solute content in range of 7075 series with marginal Sc content (0.2%) exhibited better hardening response in the temperature regime. This temperature range usually called ή-phase formation region (or peak aged region) that can be achieved with marginal solute and Sc content.In Fig.-2(c) shows at 180 ^{o}C ageing phenomena that the hardness of alloys (Alloy-1 & Alloy-2) peak hardening reached in 1 h and 6 h ageing times, respectively. Because in alloy-1 solute content in the range of 7075 series and in alloy-2 solute content high these two factors are enable to exhibited hardening effect even at 180 ^{o}C ageing treatment.This temperature range usually called η($MgZn_2$)-phaseformation region in overall ageing phenomena.The micrograph shown in Fig.-3(a) (TEM analysis) represents some area with an unusually high number density of precipitates and most of precipitates along the grain boundary are embedded. In alloy-1, in presence of fine precipitates like GP-zones spotted inside ring of diffraction patterns as well as fcc Al solid solution. Similarly, in Fig.-3(b) represents some hump-type regions and small precipitates on grain boundary, which indicates the presence of the Al_3Sc phase distribution observed [8].In Fig.-4(a-b), activation energies, E_a (kJ/mole)calculation based on ageing temperature and time from the Arrhenius equation. It is observed for precipitation reactions within the temperature range 120-180 ^{o}C. In graphical curve of ln(ΔHV) vs. 1/T (^{o}K) gives a straight line with a slope of E_a/R, R is gas constant, (8.314 J/mole.K). The activation energy of precipitation can be measured by the following the changes the hardness with temperature and using the Arrhenius relationship, i.e., $\Delta HV=\Delta HV_0 \exp(-E_a/RT)$. By plotting ln(ΔHV) vs. 1/T, the slope of the linear regression fitting will be – E_a/R, and the constant ΔHV_0 can be calculated from the intercept with the vertical axis of the linear regression line [12,13].The activation particles which have forming during decomposition of the supersaturated solid solution. The activation energy values were in general found to increase with increasing ageing time in present studies alloys (in Table-3). For alloy-3 the low activation energyindicates that, the driving force of the cluster process is low which implies that, the Sc addition to this alloy enhances the clustering process.The engineering stress-strain curves (in Fig.-5) are based onload-extension curves which generat-

(a)

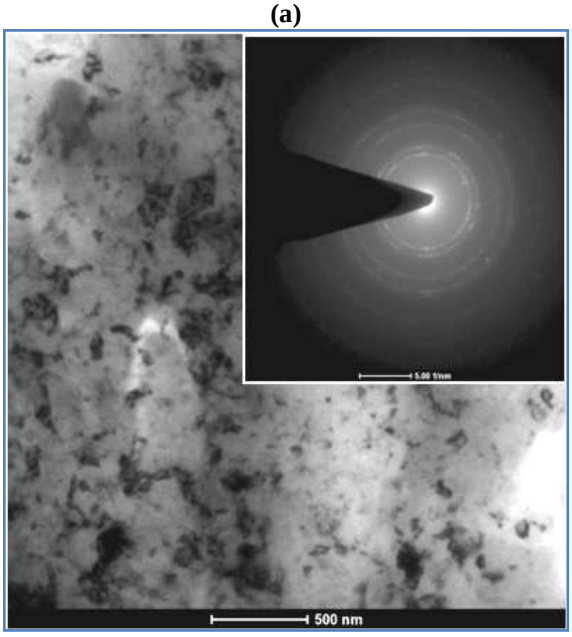

(b)

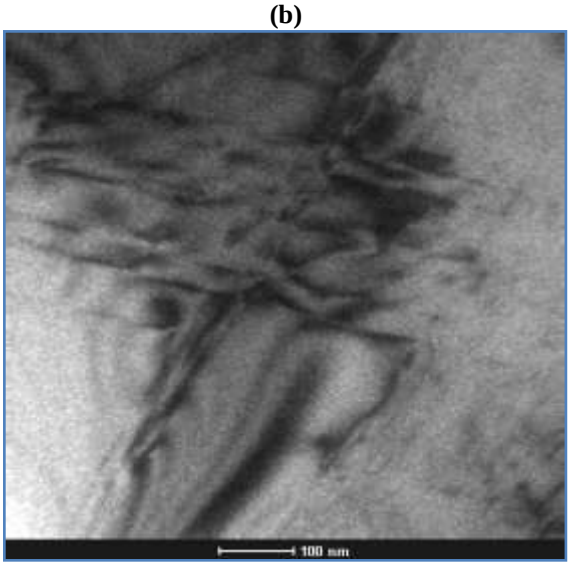

Fig.-3: TEM micrograph with inside diffraction pattern in as-cast condition (a) Alloy-1; (b) TEM micrograph of Alloy-3.

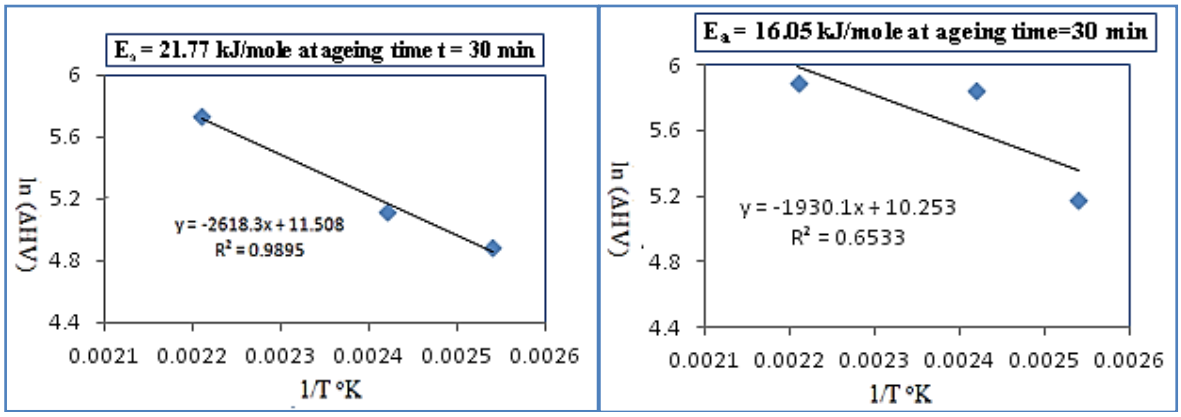

Fig.-4: Activation energy graphs of: (a) Alloy-1&(b) Alloy-2 for 30 min ageing period.

Table-3: Activation energies, E_a (kJ/mole)calculation based on ageing temperature and time from the Arrhenius equation.

Alloy no.	Values of activation energies, E_a (kJ/mole); at ageing time (h)				
	0.5 h	2 h	6 h	10 h	16 h
Alloy-1	21.77	20.61	19.94	13.86	3.58
Alloy-2	16.05	14.62	10.41	9.79	6.79
Alloy-3	1.07	5.99	4.65	7.42	6.79
Alloy-4	16.09	16.58	18.86	23.73	22.88

edduring uniaxial tensile testing in Instron Universal Testing Machine. The tensile samples are made as per FSP method (in Fig.-1) and standard dimensions (gauge length × width × thickness = 26 mm × 4 mm × 2.5 mm) are maintained. At instance, tensile test results are tabulated in Table-4 of two categories of samples: set-1solution treated conditionand noFSP; other set-2 solution treated + FSP samples. In Fig-5from set-2 of samples exhibited tensile properties,where 0.2% proof stress (instead of yield stress for Al-alloys), ultimate tensile stress, andelongation increased many fold, because during FSP cast inhomogeneties, porosityare eliminated due to

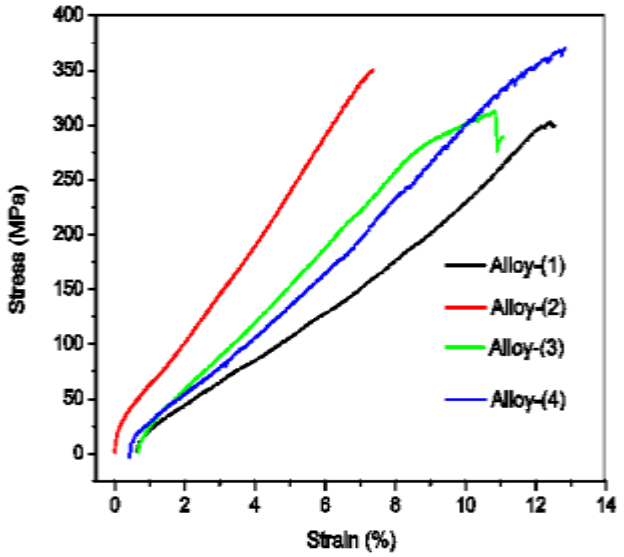

Fig.-5: Engineering Stress-Strain curves (at T_4+FSP condition) of studies Alloys.

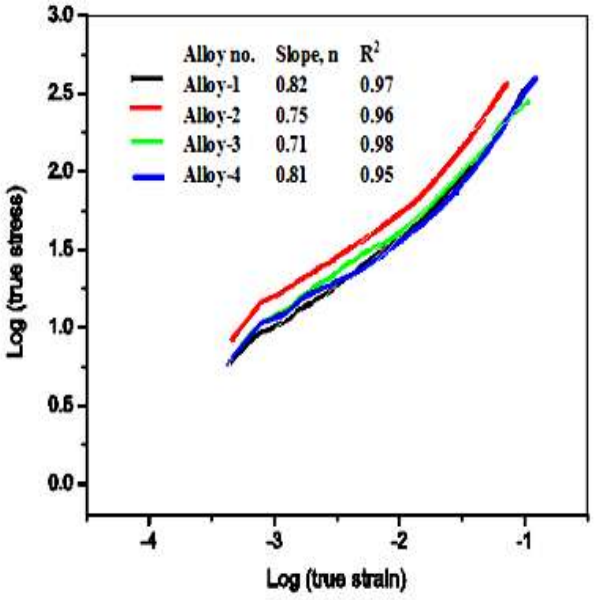

Fig.-6: Log-log plot of true stress-true strain curves of studies Alloys.

intense plastic deformation and frictional heat to generation of dynamic recrystallization, producing fine and equiaxed grains in the stirred zone. In Fig.-6, illustration has been carried out from the slope of the log (true stress) vs log (true strain) plots; the strain hardening exponents were calculated. In addition, from equation-1 can be solved n (strain hardening exponent) values, which are indicated marginally high (tabulated in Table-4)for all alloys [14].The

hardness measurements along the FSP zone also indicated good surface hardening for studies alloys[in Table-4]. It can be concluded that the larger n values to higher tougher materials. So, to characterize the deformation mechanism, true stress-true strain of engineering stress-engineering strain curves are generally used. It is generally attributed to a dynamic strain ageing process which occurs when solute atoms are diffusing sufficiently rapidly to slow down dislocations, moving under the action of an applied stress by forming 'atmospheres' around them. For the interstitial solutes, serrated yielding may be observed during testing at close to room temperature. For substitutional solutes the effects are normally seen only at elevated temperature, unless diffusion has been artificially accelerated, for example: by quenching from a high temperature to retain excess vacancies, or by generating vacancies during plastic deformation.Therefore, the analysis of the deformation simply based on engineering stress-engineering strain and true stress- true strain curves. Moreover, the Al-Zn-Mg alloys close in composition to that produced commercially can be made to exhibit good-plasticity by the addition of Sc as a grain-refining element and further enhancement of surface modification by FSP [15].

Table-4: Results of tensile properties, hardness and their values of strain hardening.

Alloy no.	T_4 condition			T_4 + FSP condition (FSP proceed by double passes)			$HV_{10kg.}$(at FSP region of avg.10 indentations)	Strain hardening, n
	$\sigma_{0.2}$(MPa)	σ_u(MPa)	δ(%)	$\sigma_{0.2}$(MPa)	σ_u(MPa)	δ(%)		
Alloy-1	23.2	35.1	1.6	123.4	242.4	9.3	153.0	0.82
Alloy-2	51.4	93.6	2.1	154.8	316.8	6.6	167.0	0.75
Alloy-3	53.7	83.9	3.6	162.1	278.1	9.1	141.8	0.71
Alloy-4	72.0	120.0	4.1	165.8	325.4	11.1	160.6	0.81

*N.B: T_4 = Solutionized at 465 ^oC/1 h then WQ; yield strength denoted at 0.2% offset from stress-strain curve.

IV. Conclusions

1. Too much addition of low solubility transition metal will lead to a low age-hardenability.
2. The addition of Sc to aluminium alloys leads to formation of Al_3Sc precipitates produce a significant hardening effect. The lattice mismatch between Al_3Sc and aluminium matrix is ~1.4%.
3. The TEM investigation revealed that the precipitation hardening particles as well as the precipitation of Al_3Sc particles.
4. The maximum activation energy (E_a) has been found out at increasing ageing time from 16.09 to 22.98 kJ/mol for alloy-4. On the other hand, for alloy-3 exhibited lower activation energy indicates that, the driving force of the precipitation process is low, because the Sc addition to this alloy enhances the precipitation process.
5. The higher ductility is due to the elimination of porosity and the breakup of cast inhomogenities. The tensile strength after FSP has been improved due to grain refinement and homogenisation of precipitates particles as well as secondary Al_3Sc particles of studied alloys.
6. The strain hardening exponent, n has been calculated from logarithmic true stress-true stain curves. Values indicated that thematerials havegood toughness.

References

[1.] H. Loffler, I. Kovacs, J. Lendvai, Journal of Materials Science 18 (1983) 2215-2240.
[2.] C. Watanabe, D. Watanabe, R. Monzen, Materials Transactions, Vol. 47, No.9 (2006) pp. 2285-2291.
[3.] J. Royset, N. Ryum, International Materials Reviews, Vol. 50, No. 1, 2005, 19-44.
[4.] T. Torma, E. Kovacs-Csetenyi, T. Turmezey, T. Ungar, I. Kovacs, Jr. of Materials Science, 24(1989) 3924-3927.
[5.] A. Juhasz, P. Tasnadi, N.Q. Chinh, I. Kovacs, Jr. of Materials Science, 22(1987) 3679-3684.
[6.] S. Miura, T. Mimaki, S. Moriwaki, N. Ono, Materials Transactions, Vol. 49, No. 11 (2008) pp. 2709-2713.
[7.] C.J. Hsu, P.W. Hao, N.J. Ho, ScriptaMaterialia 53(2005) 341-345.
[8.] Y.X. Gan, D. Solomon, M. Reinbolt, Materials, 2010, 3, 329-350.
[9.] R. Ferragut, ActaPhysicaPolonica A, Vol. 107 (2005). No. 5, pp. 776-783.
[10.] J.D. Embury, R.B. Nicholson, ActaMetallurgica, Vol. 13, April 1965,pp. 403-417.
[11.] Y. Milman, Materials Sc. Forum, Vols. 519-521 (2006) pp. 567-572.

[12.] W.Sha, Physica Status Solidi(a) 203, No. 8, (2006) 1927-1933.
[13.] W. Sha, Materials and Design, 28 (2007) 1524-1530.
[14.] J. E. King, C.P. You, J.F. Knott, ActaMetallurgica, Vol. 29, 1981, pp. 1553-1566.
[15.] N. Kumar, R.S. Mishra, Proc. Of the 5th Annual ISC Research Symposium ISCRS 2011 April 7, 2001, Rolla, Missouri, pp. 1-8.